Geotextiles and Geomembranes 28 (2010) 536–546

Contents lists available at ScienceDirect

Geotextiles and Geomembranes

journal homepage: www.elsevier.com/locate/geotexmem

Properties of geosynthetics exhumed from a final cover at a solid waste landfill

Craig H. Benson [a,*], I. Emre Kucukkirca [b], Joseph Scalia [a]

[a] Geological Engineering, University of Wisconsin, Madison WI 53706, USA
[b] Shannon and Wilson, Seattle WA 98103, USA

ARTICLE INFO

Article history:
Received 15 March 2009
Received in revised form
27 February 2010
Accepted 1 March 2010
Available online 3 April 2010

Keywords:
Geosynthetics
Degradation
Landfill final cover
Field condition
Reduction factor

ABSTRACT

Samples of geocomposite drain (GCD), geomembrane (GM), and geosynthetic clay liner (GCL) were exhumed from a final cover at a solid waste landfill to assess their condition after 4.7–5.8 yr of service. Permittivity of the GCD diminished by a factor of 3.9, but the transmissivity was higher than published by the manufacturer. Ply adhesion of the GCD diminished by a factor of 2.0. Geonet ribs in the geocomposite drain (GCD) contained a light coating of fines and plant roots, but there was no evidence of significant clogging. The geotextile on the upper surface of the GCD met the commonly used criterion for filtration (AOS < 0.6 mm for adjacent soil with <50% fines), indicating that this filtration criterion was satisfactory. Tensile yield strength of the GM diminished by a factor of 1.2, but the melt flow index was unchanged and the oxidation induction time exceeded the manufacturer's specification. GCD-geomembrane interface strength appeared unchanged. Four GCL samples had hydraulic conductivities 1000–10,000 times higher than the hydraulic conductivity measured during construction, whereas hydraulic conductivity of the other seven samples was practically unchanged. Based on these observations, the following reduction factors are suggested for installation damage and near-term service conditions (<6 yr) for the geosynthetics used at this site: GCD permittivity or transmissivity – 4.0, GCD ply adhesion – 2.0, geomembrane tensile strength – 1.5, and GCD-geomembrane interface friction – 1.0. No recommendation is made regarding a factor for the hydraulic conductivity of GCLs.

1. Introduction

Final covers employing geosynthetic materials are widely used for closure of modern engineered landfills. Large advances in our understanding of the engineering properties of new geosynthetics for waste containment have been made over the last two decades. However, limited information exists regarding the in-service properties of geosynthetics in waste containment systems, particularly in systems where known failures have not occurred (Eith and Koerner, 1997; Reitz and Holtz, 1997; Rowe et al., 2003). This information is important because the engineering properties of geosynthetics may be affected by factors such as installation damage, freezing, wetting and drying, biota intrusion, and sustained normal and shear stresses under conventional in-service conditions. Understanding the in-place properties of geosynthetics used in final covers, and if these properties differ from those measured or anticipated during design, is important to ensure that final covers function as expected.

In 2007, a large portion of the final cover on a solid waste landfill in Wisconsin, USA was removed as part of a vertical expansion. The cover, which was constructed in 2001 and 2002, employed a composite barrier consisting of a geomembrane (GM) overlying a geosynthetic clay liner (GCL). A geocomposite drain (GCD) was directly above the composite barrier. All of the geosynthetics were installed according to the construction quality control standards required in the Wisconsin Administrative Code. Removal of the cover provided a unique opportunity to collect samples and measure the engineering properties of the geosynthetics after they were in service for as long as 5.8 yr.

Samples of each geosynthetic material were collected and tested in the laboratory for typical engineering properties employed during design. These properties included the tensile strength of the GM, the interface strength between the GM and GCD, the transmissivity and permittivity of the GCD, and the hydraulic conductivity of the GCL. Apparent opening size tests were conducted to evaluate fouling of the geotextile on the GCD and melt flow index and oxidation induction time tests were conducted to evaluate degradation of the GM polymer. When possible, comparisons were made between properties of the exhumed geosynthetics and those measured for construction quality control. ASTM standard test methods were used to minimize bias between test data from the

* Corresponding author. Tel.: +1 608 262 7242; fax: +1 608 890 37181.
E-mail addresses: chbenson@wisc.edu (C.H. Benson), iek@shanwil.com (I.E. Kucukkirca), scalia@wisc.edu (J. Scalia).

0266-1144/$ – see front matter © 2010 Elsevier Ltd. All rights reserved.
doi:10.1016/j.geotexmem.2010.03.001

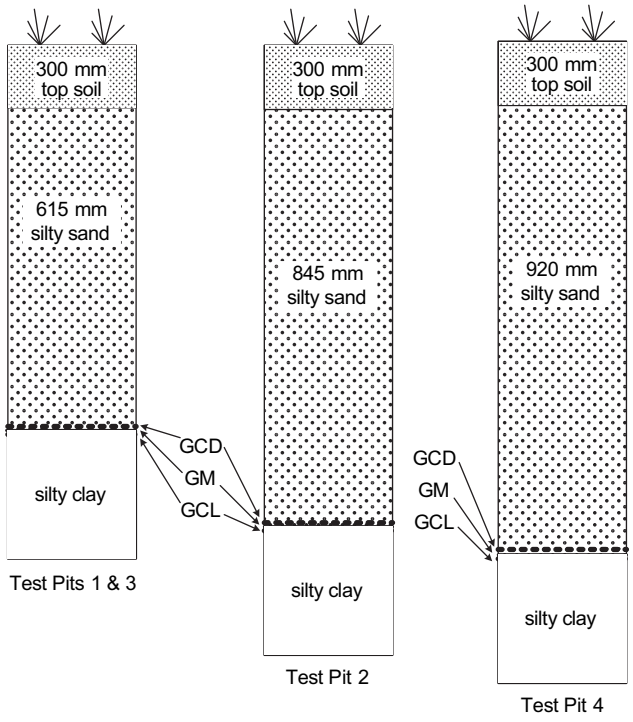

Fig. 1. Profiles of the final cover observed in Test Pits 1 though 4. GCD = geocomposite drain, GM = geomembrane, and GCL = geosynthetic clay liner.

exhumed samples and data collected during testing of the geosynthetics during construction.

This paper describes the cover profile that was exhumed, observations made during the exhumation process, and engineering properties of the exhumed geosynthetics. Recommendations are also made regarding site-specific reduction factors for design calculations (i.e., factors applied to engineering properties of new geosynthetics during design to reflect changes in the properties that occur while geosynthetics are in service).

2. Exhumation

Four test pits were excavated in the final cover in June 2007. Test Pits 1 and 2 were excavated on an eastern side slope (4:1 slope) and Test Pits 3 and 4 were excavated on the top deck (3% slope). Soils over the geosynthetics were removed from an area approximately 4 × 4 m using a tracked excavator until the excavation was within approximately 150 mm of the uppermost geosynthetic layer. The remaining soil was removed by hand.

A schematic of the final cover profile observed in test pits is shown in Fig. 1. The final cover consists of (top–bottom) a surface layer of top soil (300 mm), a silty sand (615–920 mm) protective layer, a geocomposite drain (GCD), a geomembrane (GM), and a geosynthetic clay liner (GCL). The GCL was placed on top of a layer of fine-grained subgrade. General characteristics of the geosynthetics exhumed from the test pits are summarized in Table 1.

Bulk soil samples were collected from soil layers directly adjacent to the geosynthetics (protective layer and subgrade) for particle size analysis. Ionic strength and relative abundance of monovalent and divalent cations in the pore water of the subgrade were determined using the batch elution method in ASTM D 6141 (*Standard Guide for Screening Clay Portion of Geosynthetic Clay Liner (GCL) for Chemical Compatibility to Liquids*, ASTM, 2007). Particle size distributions of the soils are shown in Fig. 2. Similar soils were present in each layer in all four test pits. The protective layer was comprised of clayey sand with a USCS designation of SP–SC, whereas the subgrade was a silty clay with a USCS designation of CL–ML. Water content of the subgrade, which was in direct contact with the GCL, fell within a narrow range (14.5–16.2%, Table 2), with a median of 15.4%. Chemical characteristics of the subgrade pore water are also summarized in Table 2. The pore water is dominated by divalent cations (RMD $\ll$ 1 $M^{0.5}$), which is characteristic of most cover soils (Meer and Benson, 2007; Benson and Meer, 2009).

After the top soil and protective layer were removed, rectangular samples (2 × 2 m) of the GCD were removed from the floor of the test pit by cutting the perimeter with a sharp utility knife. The samples were wrapped in plastic for transport. Samples of geomembrane were then removed in a similar manner. Three smaller samples of GCL (0.3 × 0.3 m) were collected from each test pit using the procedure described in ASTM D 6072 (*Standard Practice for Obtaining Samples of Geosynthetic Clay Liners*, ASTM, 2007). The GCLs were slid onto rigid PVC panels during sampling to prevent flexure during transport and sealed with plastic to prevent loss of moisture. All GCL samples were placed in plastic containers on a 100-mm-thick bed of sand and were covered with at least 300 mm of soil to apply confining pressure during transport and storage. All of the exhumed geosynthetic samples were transported by truck to the University of Wisconsin–Madison (UW) for evaluation and testing.

Table 1
Description of geosynthetic materials and characteristics of cover in test pits.

Test Pit	1	2	3	4
Location	Lower Side Slope	Upper Side Slope	Top Deck	Top Deck
Installation Date	8/2001	8/2001, 9/2002	9/2002	9/2002
Sampling date	6/2007	6/2007	6/2007	6/2007
Service life (years)	5.8	4.7, 5.8	4.7	4.7
Surface layer thickness (mm)	915	1145	915	1220
Geocomposite drain	GSE HyperNet 5.1-mm HDPE drainage net with 227-g nonwoven, polypropylene geotextile heat-bonded both sides	GSE HyperNet 5.1-mm HDPE drainage net with 227-g nonwoven, polypropylene geotextile heat-bonded both sides	GSE HyperNet 5.1-mm HDPE drainage net with 170-g nonwoven, polypropylene geotextile heat-bonded both sides	GSE HyperNet 5.1-mm HDPE drainage net with 170-g nonwoven, polypropylene geotextile heat-bonded both sides
Geomembrane	GSE 1-mm textured LLDPE	GSE 1-mm textured LLDPE	GSE 1-mm textured LLDPE	GSE 1-mm textured LLDPE
Geosynthetic clay liner	CETCO Bentomat ST - with 5.1 ± 0.3 kg/m^2 granular bentonite	CETCO Bentomat ST - with 5.1 ± 0.3 kg/m^2 granular bentonite, Bentofix NSL – 4.7 ± 0.4 kg/m^2 granular bentonite	Bentofix NSL – 4.7 ± 0.4 kg/m^2 granular bentonite	Bentofix NSL – 4.7 ± 0.4 kg/m^2 granular bentonite

Notes: All geosynthetic products were purchased in the United States. Mean and standard deviation of bentonite mass per area from quality assurance and quality control tests conducted during installation according to ASTM D 5261.

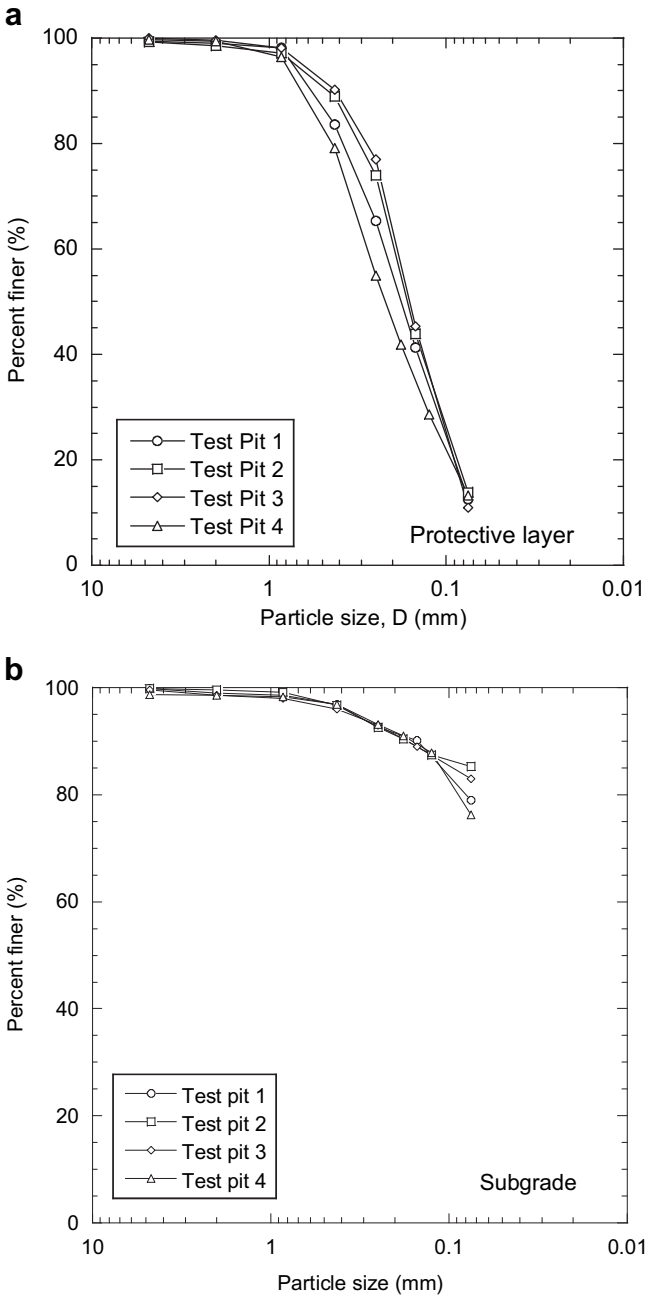

Fig. 2. Particle size distributions of the protective layer (a) and subgrade (b).

None of the geosynthetic materials had visible defects. Seams joining the GCD panels were flat and stitches bonding the geotextiles appeared to be un-weathered (Fig. 3). The geotextile was effective in retaining the overlying soil, as the overlapped areas were free of soil penetration (Fig. 3b). Roots extended throughout the soil profile, and were present in the geonet component of the GCD (Fig. 4). However, no roots were found beneath the geomembrane. A light coating of fines was present on the geonet ribs, but there was no indication of severe clogging. Geomembrane seams (Fig. 5) and GCL overlaps (Fig. 6) appeared similar to conditions typically observed during installation. No distortion or separation of the GCL was observed. Alignment of the GCLs followed the match points provided by the manufacturer (Fig. 6a), suggesting no movement of the GCL after placement. Hydrated supplemental bentonite was also present in each overlap (Fig. 6b).

Table 2
Physical and chemical properties of subgrade.

Test Pit	Water Content (%)	Percent Fines	USCS Designation	Ionic Strength (M)	RMD ($M^{1/2}$)
1	15.1	79	CL–ML	0.003	0.038
2	14.5	85	CL–ML	0.005	0.032
3	15.8	83	CL–ML	0.003	0.035
4	16.2	76	CL–ML	0.003	0.034

Note: RMD $= M_m/\sqrt{M_d}$, where M_m = total molarity of monovalent cations and M_d = total molarity of multivalent cations.

3. Laboratory methods

3.1. Geocomposite drain

3.1.1. Hydraulic properties

Permittivity of the GCD was measured following the constant head procedure in ASTM D 4491 (*Standard Test Methods for Water Permeability of Geotextiles by Permittivity*, ASTM, 2007). Prior to testing, loose soil on the surface of the GCD was removed with a brush. However, soil embedded in the geotextile was left in place. Tests were conducted with a head of 50 mm to provide a direct comparison with measurements conducted during construction and with a 10 mm head to represent a more realistic in-service

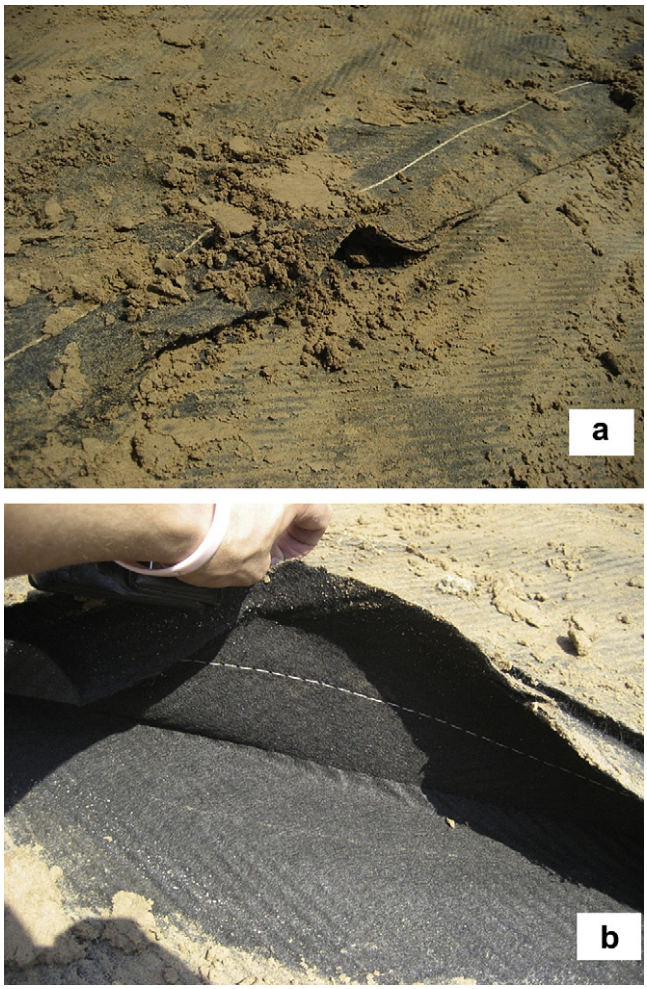

Fig. 3. Seam joining geotextiles in adjacent GCD panels in Test Pit 1: (a) seam after removing cover soil (fish mouth in middle is due to disturbance during excavation) and (b) close up showing stitching of geotextiles and clean geotextiles in the overlap.

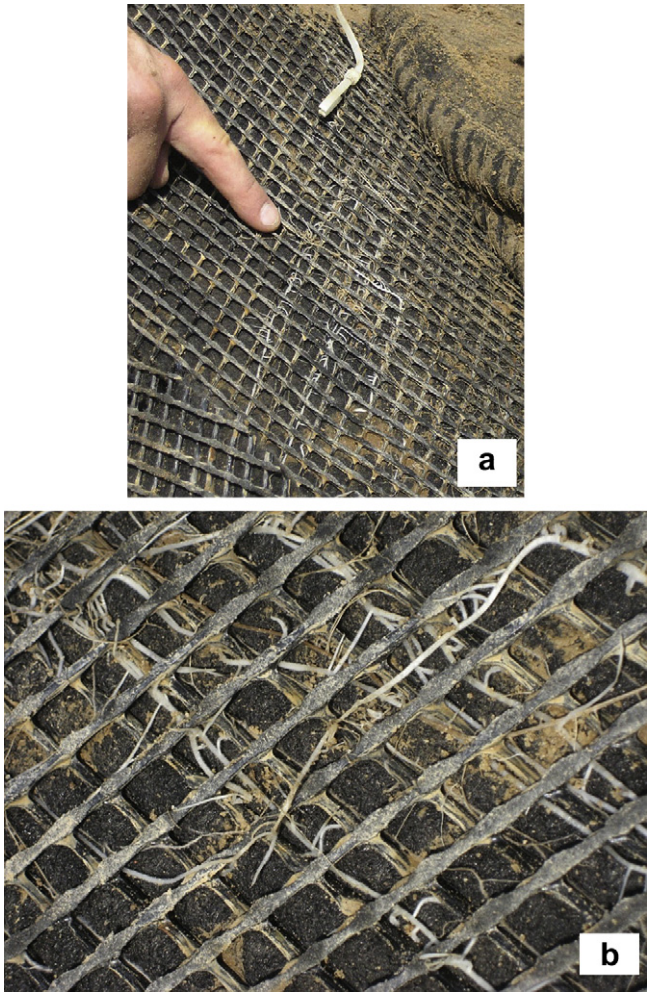

Fig. 4. Roots in the GCD and fines coating the ribs of the geonet in Test Pit 1: (a) overview and (b) close up.

Fig. 5. Examples of seams observed during exhumation: (a) dual-track wedge well uncovered in Test Pit 4 and (b) extrusion well to boot for gas well near Test Pit 4.

condition. Circular specimens (50 mm diameter) were punched from the bulk field samples using a hydraulic press. De-aired deionized (DI) water was used as the permeant liquid.

Transmissivity of the GCD was measured in the machine direction using a hydraulic gradient of 1.0 in accordance with the procedure in ASTM D 4716 (*Standard Test Method for Determining the (In-plane) Flow Rate per Unit Width and Hydraulic Transmissivity of a Geosynthetic Using a Constant Head*, ASTM, 2007). Test specimens (305 × 356 mm) were cut from the GCD samples using a razor knife. Tests were conducted using normal stresses of 24 kPa and 480 kPa. The lower normal stress was applied to simulate the in-service condition assuming that the unit weight of the overlying cover soils was 20 kN/m^3. The higher normal stress was used to obtain data that could be compared to the transmissivity published by the GCD manufacturer. Transmissivity of the GCD was computed as the quotient of the flow rate per unit area and the unit hydraulic gradient.

3.1.2. Ply adhesion

Ply adhesion of the GCD was measured using the procedure in ASTM D 7005 (*Standard Test Method for Determining the Bond Strength (Ply Adhesion) of Geocomposites*, ASTM, 2007). Loading was conducted with a screw-driven MTS Sintech 10/GL load frame equipped with Curtis Geo-Grips (load capacity = 44.5 kN) using a cross-head speed of 300 mm/min. All tests were conducted in the machine direction. Test specimens (100 × 200 mm) were prepared with a hydraulic press. Five specimens were tested from each sample, with both sides of each specimen being tested. TRI Environmental Inc. (TRI) of Austin, TX, USA conducted replicate tests on a portion of the samples.

3.1.3. Apparent opening size of geotextile

Apparent opening size of the geotextile was measured following the procedure in ASTM D 4751 (*Standard Test Method for Determining Apparent Opening Size of a Geotextile*, ASTM, 2007). All AOS tests were conducted by TRI.

3.2. Geomembrane

3.2.1. Tensile strength

Tensile strength of the geomembrane was measured using the procedure described in ASTM D 638 (*Standard Test Method for Tensile Properties of Plastics*, ASTM, 2007) so that a direct comparison could be made with construction quality control (CQC) data. All tests were conducted in the machine direction using the same load frame and grips employed for ply adhesion testing. The cross-head speed was set at 51 mm/min. Test specimens were punched from samples using a hydraulic press.

3.2.2. Interface shear strength

Interface shear strength between the geomembrane and GCD was determined following the procedure in ASTM D 5321 (*Standard*

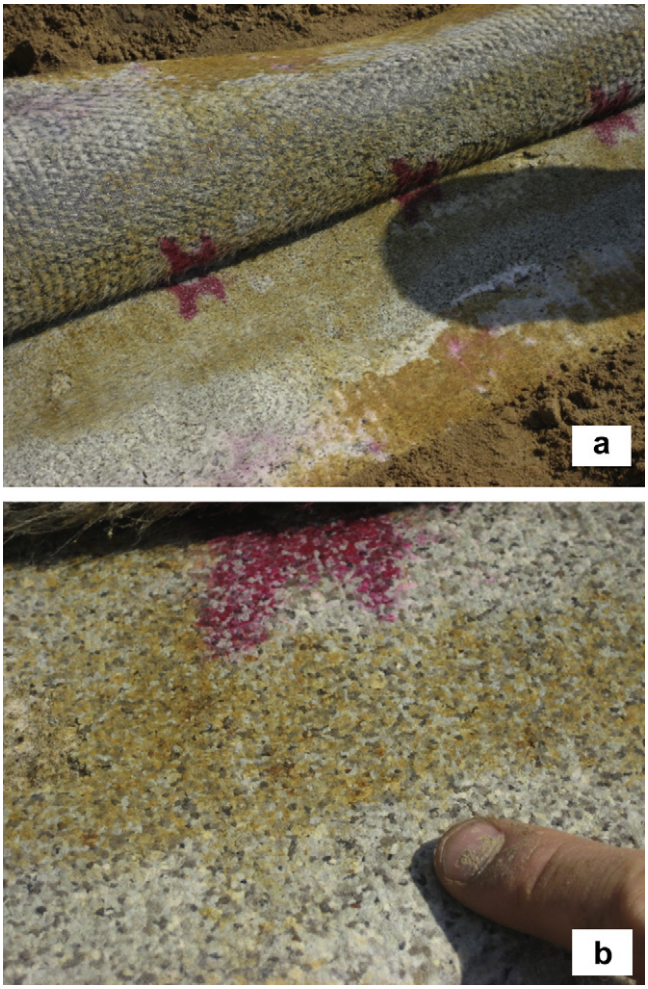

Fig. 6. GCL overlap in Test Pit 3: (a) match point along marks on original product and (b) close up showing hydrated bentonite granules in the overlap.

Test Method for Determining the Coefficient of Soil and Geosynthetic or Geosynthetic and Geosynthetic Friction by the Direct Shear Method, ASTM, 2007) using a displacement rate of 1 mm/min. Normal stresses between 12 and 50 kPa were applied to bracket conditions existing in the field. A minimum of three specimens were tested from each test pit. All specimens were cut from the exhumed samples using a razor knife (300 × 400 mm).

3.2.3. Polymeric properties

Melt flow index (MFI) and oxidation induction time (OIT) of the geomembrane were measured following ASTM D 1238 (*Standard Test Method for Melt Flow Rates of Thermoplastics by Extrusion Plastometer*, ASTM, 2007) and ASTM D 3895 (*Standard Test Method for Oxidative-Induction Time of Polyolefins by Differential Scanning Calorimetry*, ASTM, 2007). All MFI and OIT tests were conducted by TRI.

3.3. Geosynthetic clay liner

3.3.1. Hydraulic conductivity

Hydraulic conductivity tests were conducted in flexible-wall permeameters on GCL specimens using the falling headwater-constant tailwater method. Procedures in ASTM D 5084 (*Standard Test Methods for Measurement of Hydraulic Conductivity of Saturated Porous Materials Using a Flexible-Wall Permeameter*, ASTM, 2007) were followed for all hydraulic conductivity tests. ASTM D 5084 was used because it applies to porous materials in general, including GCLs, and is intended to simulate site-specific conditions. Hydraulic conductivities obtained with D 5084 and ASTM D 6766 (*Standard Test Method for Evaluation of Hydraulic Properties of Geosynthetic Clay Liners Permeated with Potentially Incompatible Liquids*, ASTM, 2007), which is specific to GCLs, tend to be identical when the permeant liquid is a dilute solution (Jo et al., 2005). However, D 6766 is for evaluating liquids that may be incompatible with GCLs, rather than to evaluate the hydraulic conductivity to water. Thus, ASTM D 5084 is more appropriate to assess the hydraulic conductivity of GCLs to dilute solutions simulating pore water.

A 0.01 M $CaCl_2$ solution was used as the permeant liquid for all tests, as suggested in ASTM D 5084 for areas with hard tap water (e.g., Madison, WI, USA, where the laboratory tests were conducted). Similar solutions have also been used by others to evaluate exhumed GCLs.

GCL specimens were cut from the field samples using a razor knife along the outer perimeter of a steel ring with a tapered edge. All test specimens were trimmed to a diameter of 152 mm. Once the specimen was removed, geotextile fibers along the edge were trimmed with scissors and bentonite paste was applied around the perimeter to minimize the potential for sidewall leakage. After being placed in the permeameter, GCLs were hydrated for 48 h with the permeant liquid prior to hydraulic conductivity testing by opening the inflow valve with the headwater applied while keeping the outflow valve closed.

The average effective stress was set at 24 kPa to represent the *in-situ* stress applied by the overlying cover soils. The average hydraulic gradient was 125, which is higher than the gradient expected in the field, but is typical for testing GCLs. Additionally, Shackelford et al. (2000) show that varying the hydraulic gradient has a much smaller effect on the hydraulic conductivity of GCLs compared to conventional soil specimens. No backpressure was used to simulate the field condition.

Tests typically were continued for 15–45 d, although most tests met the termination criteria in ASTM D 5084 in a much shorter time period. For all tests, the hydraulic conductivity remained essentially constant from the beginning of the test.

Specimens that exhibited hydraulic conductivity greater than 10^{-9} m/s were permeated with 0.01 M $CaCl_2$ spiked with rhodamine WT dye (5 mg/L) at the end of testing to determine if sidewall leakage or preferential flow was occurring. The effluent was also monitored throughout testing for migration of bentonite particles. No indication of sidewall leakage was found and no particles were observed in the effluent.

3.3.2. Swell index and chemical properties

Swell index tests were conducted on bentonite from each GCL sample following the methods described in ASTM D 5890 (*Standard Test Method for Swell Index of Clay Mineral Component of Geosynthetic Clay Liners*, ASTM, 2007) using DI water as the test liquid. Bound cations and the cation exchange capacity (CEC) were determined following the methods described in the draft ASTM *Standard Test Method for Measuring the Exchange Complex and Cation Exchange Capacity of Inorganic Fine-Grained Soils*, which is being balloted by ASTM Subcommittee D18.04. Bound cation mole fractions were calculated as a fraction of the CEC.

4. Results and discussion

4.1. Geocomposite drain

Physical properties of the exhumed GCD are summarized in Table 3. A complete compilation of the test results is in Benson et al. (2008).

Table 3
Summary of properties of exhumed geocomposite drain. Average is reported with range in parenthesis.

Test Pit	Sample	Transmissivity (m^2/s)		Permittivity (s^{-1})		Ply Adhesion (N/m)		AOS (mm)
		$\sigma = 24$ kPa	$\sigma = 480$ kPa	10 mm head	50 mm head	UW	TRI	
TP 1	1	4.4×10^{-4}	2.0×10^{-4}	0.30	0.20	230	–	–
		(2.4×10^{-4}–6.2×10^{-4})	(1.2×10^{-4}–2.9×10^{-4})	(0.22–0.48)	(0.11–0.34)	(30–420)	–	–
	2	5.4×10^{-4}	2.3×10^{-4}	0.39	0.31	340	–	–
		(5.1×10^{-4}–5.7×10^{-4})	(2.2×10^{-4}–2.5×10^{-4})	(0.22–0.56)	(0.17–0.43)	(290–430)	–	–
	3	3.4×10^{-4}	1.4×10^{-4}	0.61	0.51	180	220	0.117
		(2.3×10^{-4}–4.3×10^{-4})	(1.0×10^{-4}–1.6×10^{-4})	(0.42–0.79)	(0.39–0.61)	(50–240)	(160–320)	(0.106–0.125)
TP-2	1	2.8×10^{-4}	1.1×10^{-4}	0.593	0.42	490	–	–
		(2.2×10^{-4}–3.3×10^{-4})	(1.0×10^{-4}–1.2×10^{-4})	(0.40–0.87)	(0.33–0.54)	(400–690)	–	–
	2	6.1×10^{-4}	1.7×10^{-4}	0.68	0.55	510	–	–
		(2.9×10^{-4}–1.1×10^{-3})	(1.2×10^{-4}–2.7×10^{-4})	(0.41–0.81)	(0.31–0.70)	(140–850)	–	–
	3	4.0×10^{-4}	1.5×10^{-4}	0.30	0.26	430	340	0.100
		(3.6×10^{-4}–4.8×10^{-4})	(1.2×10^{-4}–1.9×10^{-4})	(0.22–0.35)	(0.19–0.33)	(280–570)	(160–560)	(0.090–0.106)
TP 3	1	3.0×10^{-4}	1.2×10^{-4}	0.35	0.27	440	–	–
		(1.9×10^{-4}–4.7×10^{-4})	(7.2×10^{-5}–2.0×10^{-4})	(0.21–0.51)	(0.15–0.39)	(330–540)	–	–
	2	7.2×10^{-4}	1.4×10^{-4}	0.69	0.49	490	–	–
		(2.0×10^{-4}–1.6×10^{-3})	(9.8×10^{-5}–1.6×10^{-4})	(0.61–0.78)	(0.39–0.60)	(350–690)	–	–
	3	3.6×10^{-4}	1.3×10^{-4}	0.59	0.46	470	390	0.126
		(3.3×10^{-4}–4.2×10^{-4})	(1.2×10^{-4}–1.5×10^{-4})	(0.36–0.93)	(0.24–0.66)	(320–610)	(230–740)	(0.106–0.150)
	4	5.7×10^{-4}	1.5×10^{-4}	0.45	0.26	270	–	–
		(3.0×10^{-4}–8.9×10^{-4})	(1.2×10^{-4}–1.7×10^{-4})	(0.25–0.68)	(0.19–0.39)	(130–410)	–	–
TP 4	1	3.4×10^{-4}	1.2×10^{-4}	0.79	0.60	580	–	–
		(1.8×10^{-4}–4.5×10^{-4})	(1.5×10^{-6}–2.0×10^{-4})	(0.57–0.98)	(0.59–0.63)	(160–990)	–	–
	2	5.7×10^{-4}	1.2×10^{-4}	0.81	0.51	480	–	–
		(2.4×10^{-4}–1.3×10^{-3})	(6.1×10^{-5}–2.2×10^{-4})	(0.27–1.19)	(0.23–0.76)	(320–700)	–	–
	3	5.6×10^{-4}	1.0×10^{-4}	0.88	0.53	570	490	0.136
		(2.8×10^{-4}–1.0×10^{-3})	(7.4×10^{-5}–1.4×10^{-4})	(0.81–0.92)	(0.44–0.62)	(360–850)	(280–840)	(0.125–0.180)
	4	2.7×10^{-4}	1.3×10^{-4}	0.61	0.38	520	–	–
		(2.6×10^{-4}–3.0×10^{-4})	(1.1×10^{-4}–1.4×10^{-4})	(0.49–0.71)	(0.22–0.54)	(400–680)	–	–

4.1.1. Hydraulic properties

Permittivity of the GCD is shown in Fig. 7. The permittivity in each test pit ranged nearly one order of magnitude at 10 mm head and approximately one-half order of magnitude at 50 mm head. Samples from Test Pit 4 had slightly higher permittivity than those from the other test pits, but in general the permittivity did not vary appreciably (<50%) between test pits. In addition, there is no systematic difference between the permittivities of samples from Test Pits 1 and 2 and those from Test Pits 3 and 4, suggesting that there was no practical difference between the permittivity on the top deck and the slopes.

A direct comparison between permittivity of the exhumed GCD and the as-built condition can only be made for tests conducted with 50 mm head (tests at 10 mm head were not conducted during construction). At 50 mm head, all of the exhumed samples had permittivity lower than the permittivity measured during CQC, which ranged between 1.51 and 1.72 s^{-1} (1.61 s^{-1}, on average). Permittivity of the exhumed samples was at most 14.6 times lower, and 3.9 times lower on average, than the average as-built permittivity. Nevertheless, the permittivity of the exhumed GCD was still at least ten times higher than necessary to conduct unit gradient flow from the overlying silty sand (saturated hydraulic conductivity $<10^{-5}$ m/s, Benson et al., 2008). Reitz and Holtz (1997) report similar reductions in permittivity for four geotextiles exhumed from landfill final covers in Washington State that were in service from 5 to 9 yr.

The modest reduction in permittivity that occurred while in service was probably due to penetration of soil into the upper geotextile, which retained 18–323 g/m^2 of soil (Benson et al., 2008). AOS of the exhumed geotextile was also lower than the AOS published by the manufacturer (Fig. 8), which is consistent with retention of soil within the pores of the geotextile (i.e., soil in the pores of the geotextile reduces the AOS). Variation in the amount of soil retained within the geotextile probably was responsible for the variation in permittivity in each test pit. Roots in the geonet (Fig. 4) may also have contributed to the reduction in permittivity. However, no systematic relationship between permittivity and retained soil or presence of roots could be identified.

Transmissivity of the GCD at a hydraulic gradient of 1.0 and at confining stresses of 24 and 480 kPa is shown in Fig. 9. Within a test pit, the transmissivity varies by at most a factor of 6 (24 kPa) or 8 (480 kPa), and between test pits the average transmissivity varies less than a factor of 2. Moreover, as with permittivity, there is no systematic difference between transmissivities for samples from Test Pits 1 and 2 and those from Test Pits 3 and 4, suggesting that there is no practical difference between the transmissivity on the top deck and the side slopes.

A comparison with the as-built transmissivity could not be made, as transmissivity tests were not conducted on the GCD as part of CQC testing. However, at 480 kPa, the transmissivity of the exhumed GCD is higher than the transmissivity published by the manufacturer (4.0×10^{-5} m^2/s for the GCD in Test Pits 1 and 2; 6.0×10^{-5} m^2/s for the GCD in Test Pits 3 and 4, Fig. 9b). As noted previously, the geotextile was effective in filtering the overlying soil, as only a light coating of fines was present on the ribs of the geonet. This satisfactory filtration is consistent with the AOS of the geotextile, which met the common criterion for filtration (AOS < 0.6 mm for adjacent soils with less than 50% fines, Koerner, 1998) (Fig. 8).

4.1.2. Ply adhesion

Ply adhesion of the exhumed GCD measured at UW and TRI is shown in Fig. 10. Data sets from both laboratories fell in similar clusters. Thus, the data from both laboratories were combined for analysis.

Ply adhesion varies by as much as a factor of 6 within each test pit, with the maximum variation in Test Pit 4. Samples of the GCD exhumed in Test Pit 1 (side slope) have 2 times lower ply adhesion, on average, than those from the other test pits. However, the ply adhesion is similar in Test Pits 2–4. Thus, there is no apparent difference in ply adhesion than can be attributed to the GCD being exhumed from the side slope (Test Pits 1 and 2) or the top deck (Test Pits 3 and 4).

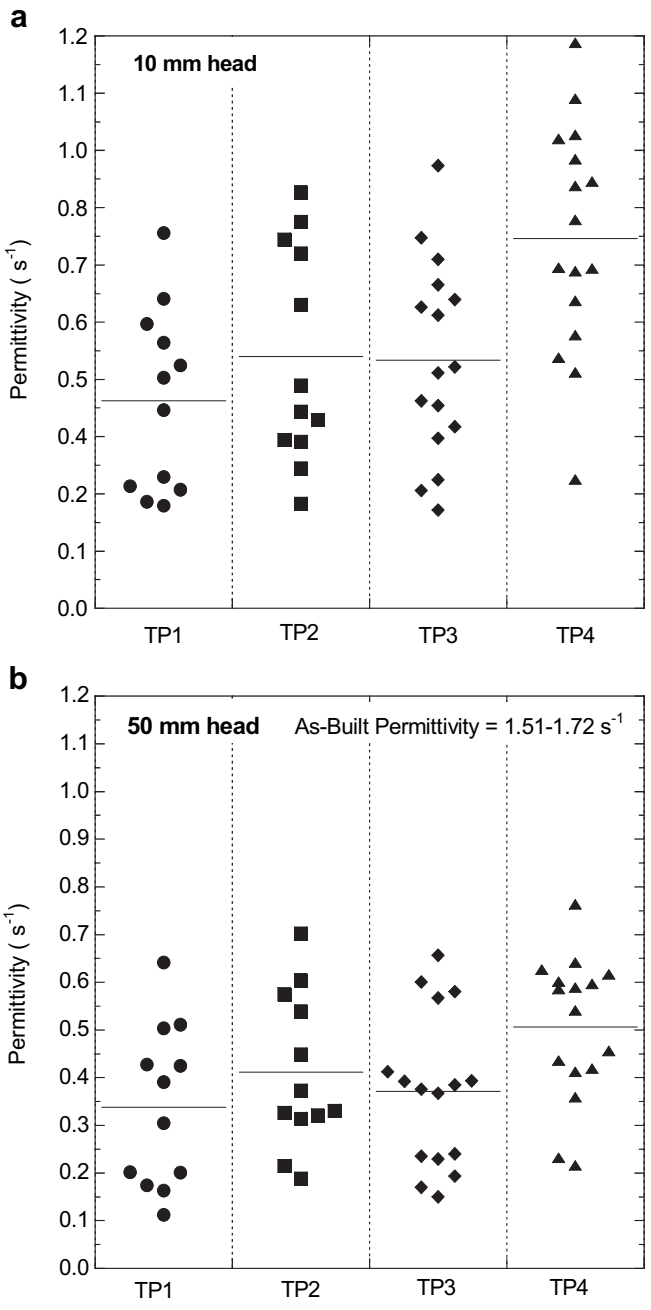

Fig. 7. Permittivity of GCD measured using 10 mm head (a) and 50 mm head (b). Horizontal bars in each column represent the average for the data in the column.

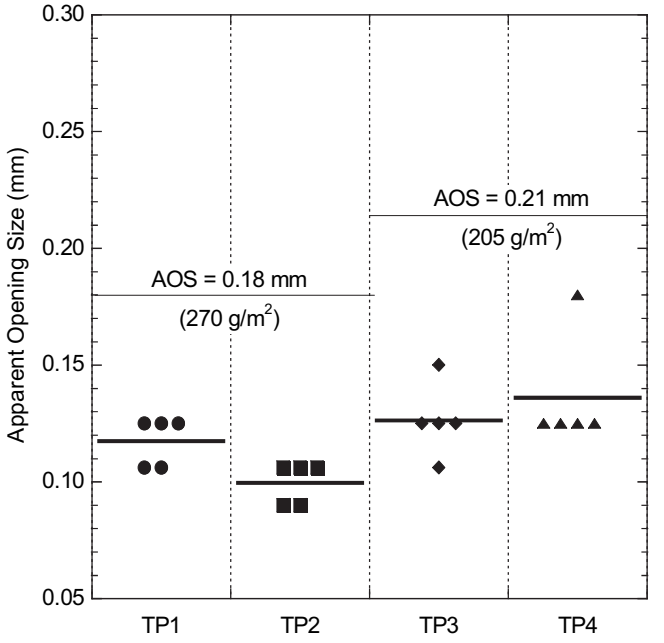

Fig. 8. Apparent opening size of the upper geotextile in the GCD. Horizontal bars in each column represent the average for the data in the column.

The average ply adhesion in each test pit is 1.7–2.2 times lower than the average ply adhesion measured during CQC (690 N/m). Inspection of specimens prior to testing showed that the bond between the geotextile and geonet had separated in some regions, and specimens with greater bond separation had lower ply adhesion. In addition, a clean separation occurred between the geotextile and geonet in the specimens with low ply adhesion (e.g., Test Pit 1, Fig. 10), suggesting that the bond between the geosynthetics in these specimens may never have been viable.

4.2. Geomembrane

4.2.1. Tensile strength

Tensile strengths of the geomembrane are shown with dot plots in Fig. 11. Average tensile strengths measured with ASTM D 638 during CQC in 2001 and 2002 are shown as horizontal lines in Fig. 11. Except for Test Pit 2, average tensile strengths of the exhumed geomembranes are lower than the average tensile strengths measured during CQC (12.2 kN/m in 2001, 14.5 kN/m in 2002). When Test Pit 2 is excluded, the average tensile strength in each test pit was a factor of 1.15–1.22 lower than the average tensile strength measured during CQC.

A definitive reason for this reduction in tensile strength was not apparent when the specimens were exhumed (e.g., they did not contain visible defects), but damage incurred during installation, exhumation, and in-service conditions may be responsible. These reductions in tensile strength apparently are not due to degradation of the polymer. MFI of the exhumed geomembranes is essentially the same as the MFI measured for manufacturer quality control (MQC) and CQC (Fig. 12), and the OIT of the exhumed geomembranes exceeded the 100 min MQC specification (Table 4).

4.2.2. Interface shear strength

Peak-strength envelopes for the GCD-geomembrane interface are shown in Fig. 13. One strength envelope was determined for each test pit. Similar interface friction angles, δ, were obtained from each pit (33–35°), but the adhesion, a, was 2 times larger for the geosynthetics exhumed from Test Pits 1 and 2 compared to Test Pits 3 and 4. Greater adhesion may have been obtained for the samples from Test Pits 1 and 2 because the GCD on the side slope contained a heavier geotextile (270 vs. 205 g/m^2, Table 1). No visible difference in texturing was evident in the exhumed geomembrane samples that could explain the differences in adhesion. Deployment on the slope (Test Pits 1 and 2) versus the top deck (Test Pit 3 and 4) probably was not responsible for the differences in adhesion.

No interface shear tests were conducted during CQC. Thus, a direct comparison between interface shear strengths of the exhumed and as-built conditions cannot be made. However, for similar materials, Stark et al. (1996) report peak interface friction angles ranging between 30 and 32° and adhesions ranging between 5 and 17 kPa. Given the similarity of the strength parameters of the

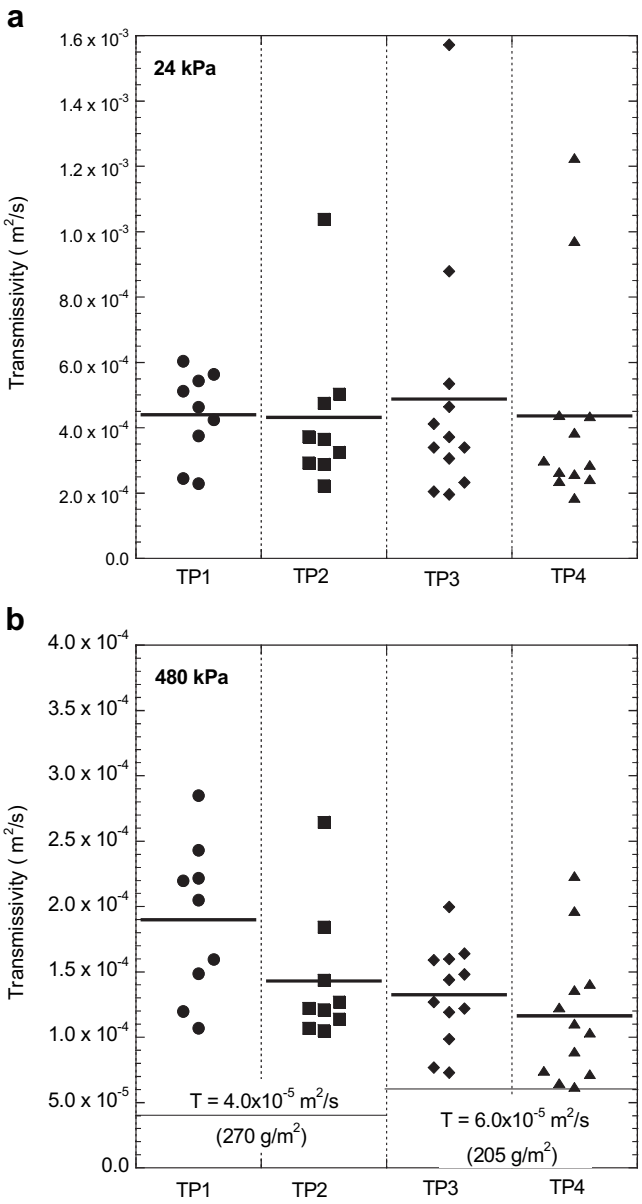

Fig. 9. Transmissivity of GCD under a normal stress of (a) 24 kPa and (b) 480 kPa. Horizontal bars in each column represent the average for the data in the column.

exhumed geosynthetics and those reported by Stark et al. (1996), no decrease in the peak interface shear strength appears to have occurred while the geosynthetics were in service.

4.3. Geosynthetic clay liner

Physical and chemical properties of the exhumed GCLs are summarized in Table 5. Data from CQC testing (QC-series data in Table 5) and from independent tests on Bentofix NSL by Meer and Benson (2007) (Meer 1 and 2 in Table 5) are also included. ASTM D 5887 (*Standard Test Method for Measurement of Index Flux Through Saturated Geosynthetic Clay Liner Specimens Using a Flexible-Wall Permeameter*, ASTM, 2007) was used to measure the hydraulic conductivity of the GCL for CQC. Meer and Benson (2007) used ASTM D 5084.

Hydraulic conductivities of exhumed GCLs are shown in Fig. 14. The average hydraulic conductivities of the GCLs in Test Pits 1 and 4

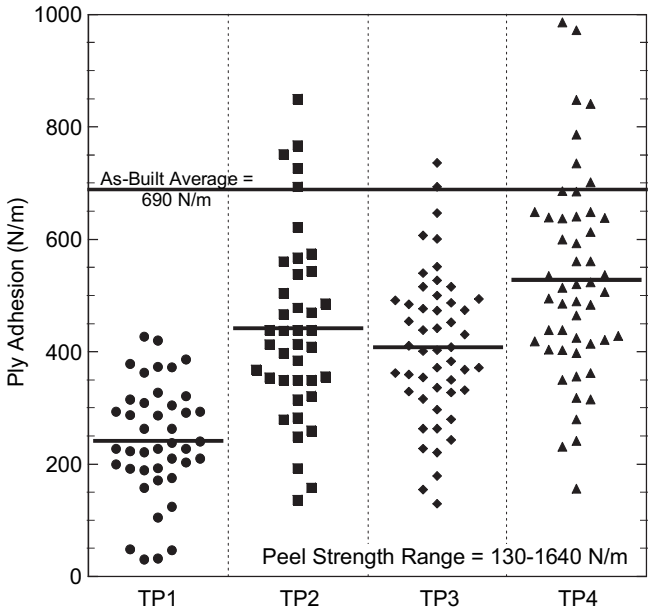

Fig. 10. Ply adhesion of GCD in each test pit. Horizontal bars in each column represent the average for the data in the column.

are similar (average = 4.2×10^{-11} and 2.6×10^{-11} m/s), even though the GCLs from these test pits represent different GCL products, installation periods (2001 vs. 2002), and service lives (4.7 vs. 5.8 yr). Additionally, the average hydraulic conductivities of the GCLs from Test Pits 1 and 4 are only slightly higher than the average hydraulic conductivity of new GCL samples measured during CQC (1.6×10^{-11} m/s) and by Meer and Benson (2007) (1.5×10^{-11} m/s). One of the GCLs exhumed from Test Pit 2 also had comparable hydraulic conductivity (average = 2.3×10^{-11} m/s) as those from Test Pits 1 and 4.

All GCLs exhumed from Test Pit 3 and one GCL from Test Pit 2 exhibited hydraulic conductivities 3–4 orders of magnitude higher than the hydraulic conductivity of the new GCL tested by Meer and

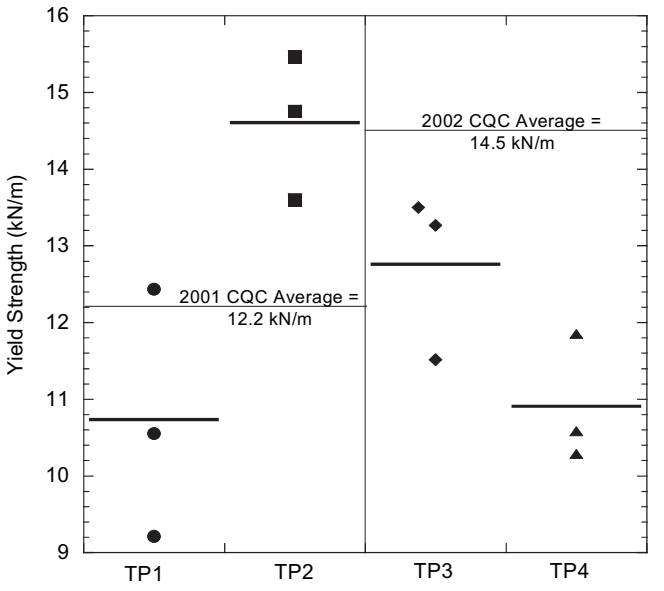

Fig. 11. Tensile yield strengths of exhumed geomembrane samples. Solid horizontal bars are average tensile strength for a given test pit.

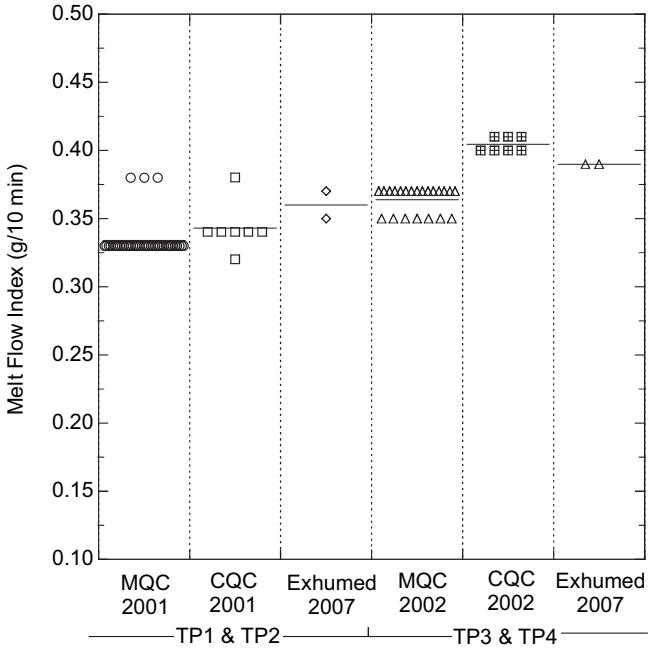

Fig. 12. Melt flow index of the geomembrane determined by the manufacturer, during CQC, and after exhumation in 2007. Horizontal bars in each column represent the average for the data in the group.

Benson (1.2×10^{-11}–1.7×10^{-11} m/s), the GCLs tested during CQC (1.2×10^{-9}–2.6×10^{-11} m/s), and the GCLs exhumed from Test Pits 1 and 4. High hydraulic conductivities were obtained for both brands of GCL, for samples from the side slope and the top deck, and for both installation periods. Thus, the GCLs with low ($<10^{-9}$ m/s) and high ($>10^{-9}$ m/s) hydraulic conductivity cannot be differentiated by sampling location, GCL product, or service life. The GCLs from Test Pits 3 and 4 were also from the same GCL panel.

Bound cations of the exhumed GCLs are summarized in Table 5. Nearly all of the original Na on the bentonite was replaced by Ca while the GCLs were in service, even though the GCLs were covered by a geomembrane. This finding is consistent with the swell indices of the exhumed GCLs (Table 5), which all fall within a narrow range (8–11 mL/2 g) characteristic of calcium bentonite (6–10 mL/2 g) (Jo et al., 2004). All swell indices of the exhumed GCLs are significantly lower than the median swell index measured during CQC (28 mL/2 g) and by Meer and Benson (2007) (35 mL/2 g). The abundant Ca in the GCL most likely is due to upward migration of divalent cations from the pore water in the underlying subgrade, which contained predominantly divalent cations (RMD = 0.032–0.038 $M^{0.5}$, Table 2).

Previous studies have shown that exchange of Ca for Na combined with dehydration can result in significant increases in the hydraulic conductivity of GCLs in landfill covers (Melchior, 1997, 2002; Cazzuffi and Crippa, 2004; Benson et al., 2007; Meer and Benson, 2007). Because all of the GCLs exhumed in this study were covered by a geomembrane that would prevent dehydration, the combined effect of Na replacement and dehydration is not a plausible explanation for the increase in hydraulic conductivity that was observed in some of the GCLs. In addition, the exhumed GCLs with low hydraulic conductivity had only slightly higher water content (58–70%) than the exhumed GCLs with high hydraulic conductivity (average = 58–63%), indicating that dehydration was modest, if it occurred at all.

Table 4
MFI and OIT of exhumed geomembrane.

Test Pit	MFI (g/10 min)	OIT (min)
1	0.35	106
2	0.37	113
3	0.39	118
4	0.39	111

Construction documentation reports for both phases of cover construction were examined to determine a cause for the unusual hydraulic conductivities of the GCLs from Test Pits 2 and 3 and to assess whether the geosynthetics were exposed for an extended period before the overlying cover soils were placed. A cause could not be identified and the elapsed time between deployment of the geosynthetics and placement of the cover soils could not be determined precisely. However, based on the construction records, the elapsed time between deployment of the geosynthetics and placement of cover soil can be bounded between 2 and 20 d.

To evaluate what mechanism might be altering the hydraulic conductivity of the GCLs, the interior of each GCL specimen was inspected after testing. Specimens that had high hydraulic conductivity contained dark vertical stains that followed bundles of needle-punching fibers (Fig. 15a). Similar stains were not present in specimens with low hydraulic conductivity. Rhodamine WT dye was coincident with these dark stains (Fig. 15b), indicating that they formed or coincided with preferential pathways through the GCL that are responsible for the high hydraulic conductivity. The darkly stained material was analyzed by X-ray diffraction and determined to be manganese oxide (MnO). Mechanisms underlying the formation of these stains are being explored (Scalia and Benson, 2010).

5. Summary and practical recommendations

Geosynthetics were exhumed in June 2007 from a final cover constructed at a solid waste landfill in Wisconsin, USA in 2001–2002. Condition of the geosynthetics was observed and tests were conducted to evaluate their engineering properties.

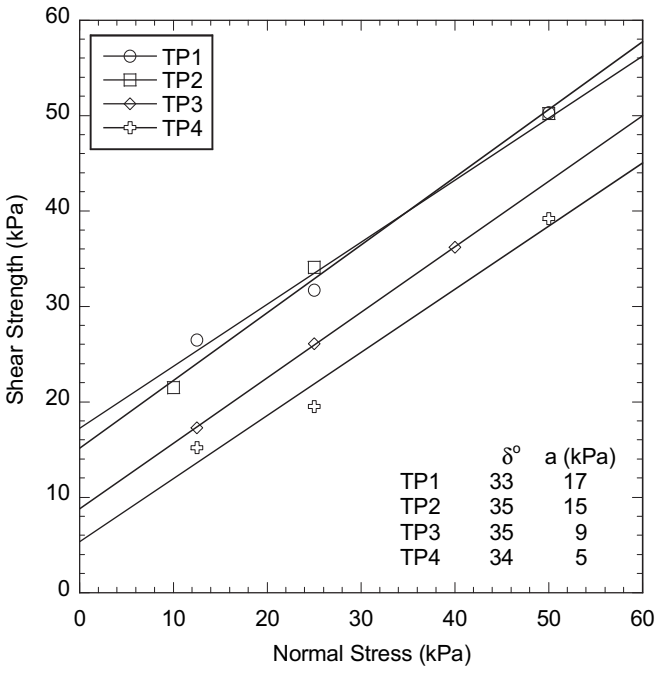

Fig. 13. Peak interface shear strength envelopes for geomembrane-GCD interface.

Table 5
Properties of exhumed GCLs.

Sample ID	Service Life (yr)	Product	Exhumed Thickness (mm)	Exhumed Dry Bentonite Mass per Unit Area (kg/m^2)	Exhumed Water Content (%)	Swell Index (mL/2 g)	Hydraulic Cond. (m/s)	Bound Cations (mole fraction)			
								Na	Ca	Mg	K
TP 2–2	5.8	Bentomat ST	6.8	4.4	58	10	1.3×10^{-8}	0.03	0.79	0.03	0.01
TP 3–1	4.7	Bentofix NSL	6.8	4.9	56	10	2.8×10^{-8}	0.01	0.78	0.01	0.02
TP 3–2	4.7	Bentofix NSL	7.2	4.8	63	11	2.1×10^{-8}	0.03	0.80	0.03	0.01
TP 3–3	4.7	Bentofix NSL	5.8	4.2	60	9	2.7×10^{-8}	0.03	0.78	0.03	0.01
TP 1–1	5.8	Bentomat ST	6.4	4.7	70	8	4.7×10^{-11}	0.04	0.79	0.04	0.01
TP 1–2	5.8	Bentomat ST	7.4	4.9	64	8	4.2×10^{-11}	0.04	0.79	0.04	0.01
TP 1–3	5.8	Bentomat ST	7.1	5.0	58	10	3.8×10^{-11}	0.03	0.78	0.03	0.01
TP 2–1	4.7	Bentofix NSL	7.8	5.0	60	8	2.0×10^{-11}	0.03	0.80	0.03	0.02
TP 4–1	4.7	Bentofix NSL	6.6	4.3	68	8	3.3×10^{-11}	0.03	0.76	0.03	0.01
TP 4–2	4.7	Bentofix NSL	6.8	4.2	67	10	3.2×10^{-11}	0.03	0.78	0.03	0.01
TP 4–3	4.7	Bentofix NSL	7.0	4.2	61	11	1.4×10^{-11}	0.03	0.80	0.03	0.02
QC–B1	New	Bentofix NSL	–	–	–	31	2.0×10^{-11}	–	–	–	–
QC–B2	New	Bentofix NSL	–	–	–	26	1.8×10^{-11}	–	–	–	–
QC–B3	New	Bentofix NSL	–	–	–	26	2.6×10^{-11}	–	–	–	–
QC–C1	New	Bentomat ST	–	–	–	30	1.5×10^{-11}	–	–	–	–
QC–C2	New	Bentomat ST	–	–	–	33	1.6×10^{-11}	–	–	–	–
QC–C3	New	Bentomat ST	–	–	–	32	1.3×10^{-11}	–	–	–	–
QC–C4	New	Bentomat ST	–	–	–	25	1.2×10^{-11}	–	–	–	–
QC–C5	New	Bentomat ST	–	–	–	25	1.3×10^{-11}	–	–	–	–
QC–C6	New	Bentomat ST	–	–	–	28	1.3×10^{-11}	–	–	–	–
Meer 1	New	Bentofix NSL	–	–	–	36	1.2×10^{-11}	0.74	0.22	0.03	0.02
Meer 2	New	Bentofix NSL	–	–	–	34	1.7×10^{-11}	0.65	0.27	0.03	0.05

Notes: Samples labeled QC-*XX* correspond to CEC tests conducted in 2001 (C1–C6) and 2002 (B1–B3). Meer 1 and Meer 2 are tests conducted at the University of Wisconsin–Madison on new samples of Bentofix NSL. Sample TP 2 was damaged during transport and was not tested.

Comparisons were made between engineering properties of geosynthetics measured during CQC and after exhumation.

No visible defects were apparent when the geosynthetics were sampled. Seams in the geocomposite drain (GCD) and the geomembrane were intact, no holes were evident in the geomembrane, and overlaps in the geosynthetic clay liner (GCL) were in proper alignment and contained hydrated supplemental bentonite. Roots were present within the drainage layer, and the geonet ribs contained a light coating of fines. However, there was no evidence that the GCD had experienced any clogging. The geotextile on the upper surface of the GCD met the commonly used criterion for filtration (AOS $<$ 0.6 mm for adjacent soil with $<$50% fines). The good filtration performance that was observed suggests that this commonly used filtration criterion was effective for the cover soils at this site, which have less than 50% fines.

Permittivity of the GCD diminished by a factor of 3.9 compared to measurements made during construction, mostly likely due to

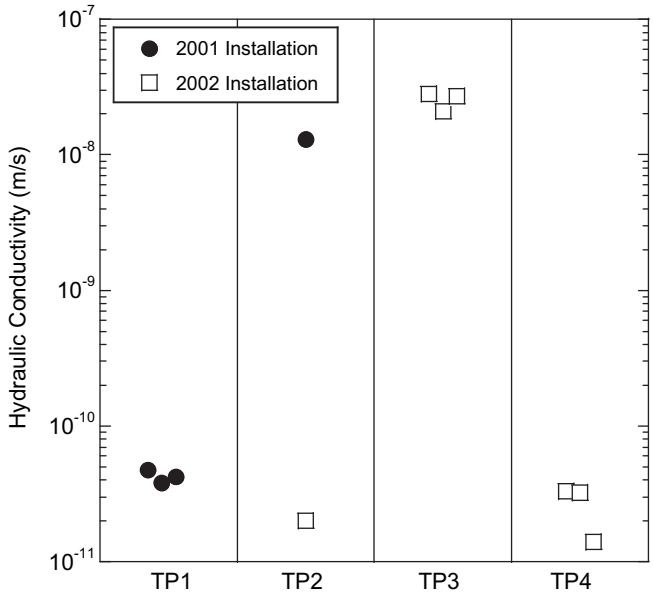

Fig. 14. Hydraulic conductivity of GCLs exhumed from Test Pits 1–4.

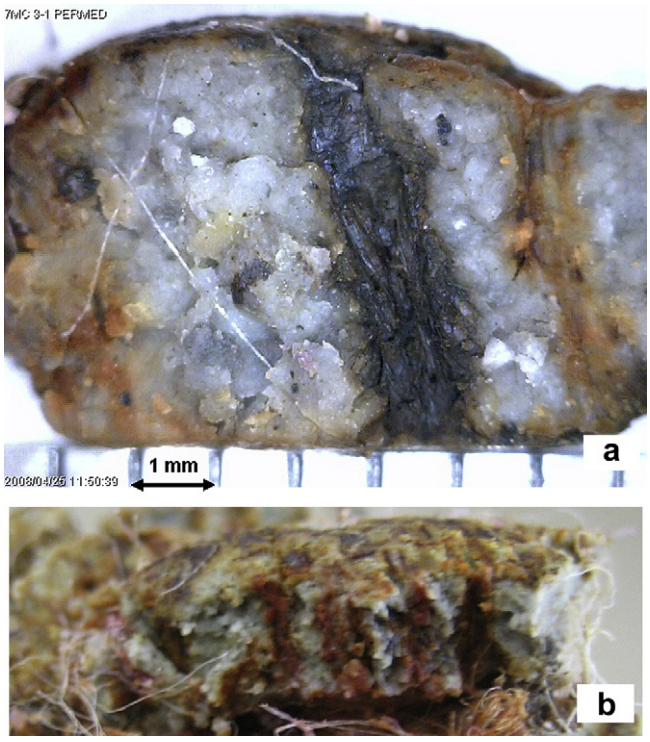

Fig. 15. Photograph in (a) is close up of the interior showing dark stain (near center) where bundle of needle-punching fibers had passed through the bentonite. Divisions along lower edge of (a) are 1-mm apart. Photograph in (b) is cross-section of GCL showing red-stained vertical streaks where preferential flow occurred along needle-punching fibers containing dark stain. Red stain is from dye added to permeant water after detecting high hydraulic conductivity. Both photographs are of GCL TP 3–1. These photographs are representative of all GCLs with high ($>10^{-9}$ m/s) hydraulic conductivity.

penetration of soil particles into the pores of the geotextile. A similar comparison could not be made for transmissivity of the GCD because transmissivity testing was not conducted during construction. However, transmissivity of the exhumed GCD was higher than the transmissivity published by the manufacturer. Ply adhesion of the GCD decreased relative to the as-built condition, and some of the bonds between the geotextile and geonet were weak. On average, the ply adhesion of the exhumed GCD was 2.0 times lower than the ply adhesion measured during CQC.

Tensile yield strength of the geomembrane diminished modestly since construction (1.2 times lower, on average, than measured during CQC). Chemical degradation of the polymer apparently was not the cause of the reduction in strength. The melt flow index of the geomembrane was virtually unchanged from the as-built condition and the oxidation induction time exceeded the manufacturer's standard for a new geomembrane. Interface strength between the GCD and the geomembrane appeared unaffected by in-service conditions.

All of the samples of the geosynthetic clay liner (GCL) exhibited essentially complete replacement of Na by Ca on the bentonite surface. However, cation exchange alone appears to have no detrimental impact on hydraulic conductivity. GCLs in two of the four test pits had hydraulic conductivities characteristic of new GCLs containing Na-bentonite. In contrast, GCLs from the other test pits had hydraulic conductivity as much as 10,000 times higher than a new GCL. These high hydraulic conductivities were caused by preferential flow along bundles of needle-punching where manganese oxide precipitated.

Data from these tests can be used to define site-specific reduction factors for design calculations. Such factors were obtained by rounding up the aforementioned average ratios of installed-to-exhumed engineering properties to the nearest 0.5. Based on this approach, the following reduction factors are recommended to account for installation damage and service <6 yr:

GCD permittivity	4.0
GCD transmissivity	4.0
GCD ply adhesion	2.0
Geomembrane tensile strength	1.5
GCD-geomembrane interface friction	1.0

The reduction factor for permittivity was assumed to apply to transmissivity (no transmissivity tests were conducted during CQC). No recommendation is being made at this time regarding a factor for the hydraulic conductivity of GCLs. More research on this issue is needed before a reliable recommendation can be made.

Acknowledgement

Financial support for this study was provided by Veolia Environmental Services (VES), the National Science Foundation (NSF Grant No. CMS-0625850), the US Nuclear Regulatory Commission, and the senior author's Wisconsin Distinguished Professorship. TRI Environmental Inc. of Austin, Texas USA provided in-kind support through complimentary laboratory testing. Gary Albee and David Marthaler of VES, Jim Olsta and Chuck Hornaday of CETCO, and Don Smith assisted with the field work. Steven Bischoff of Ayres Associates assisted in the field, prepared a topographic drawing, and provided construction quality control data from 2001 to 2002. Sam Allen and John Allen of TRI Environmental conducted the complimentary laboratory testing. Assistance provided by each of these persons is greatly appreciated. The findings and inferences in this report are solely those of the authors. Endorsement by VES, NSF, NRC, TRI Environmental, CETCO, or Ayres Associates is not implied and should not be assumed.

References

ASTM, 2007. Annual Book of Standards, Volumes 04.08, 04.13, 08.01, 08.02. ASTM International, West Conshohocken, PA.

Benson, C., Kucukkirca, I., Scalia, J., 2008. Properties of Geosynthetics Exhumed from the Seven Mile Creek Landfill Eau Claire, Wisconsin, Geo Engineering Report No. 08-22. University of Wisconsin, Madison, Wisconsin.

Benson, C., Meer, S., 2009. Relative abundance of monovalent and divalent cations and the impact of desiccation on geosynthetic clay liners. J. Geotech. Geoenviron. 135 (3), 349–358.

Benson, C., Thorstad, P., Jo, H., Rock, S., 2007. Hydraulic performance of geosynthetic clay liners in a landfill final cover. J. Geotech. Geoenviron. 133 (7), 814–827.

Cazzuffi, D., Crippa, E., 2004. Behavior vs. time of geosynthetic clay liners sampled from a Brownfield in Southern Italy after seven years of installation. GeoAsia 2004. In: 3rd Asian Regional Conference on Geosynthetics: Now and Future of Geosynthetics in Civil Engineering, Seoul, Korea, pp. 480–487.

Eith, A., Koerner, G., 1997. Assessment of HDPE geomembrane performance in a municipal waste landfill double liner system after eight years of service. Geotext. Geomembranes. 15, 277–289.

Jo, H., Benson, C., Edil, T., 2004. Hydraulic conductivity and cation exchange in non-prehydrated and prehydrated bentonite permeated with weak inorganic salt solutions. Clays. Clay. Miner. 52 (6), 661–679.

Jo, H., Benson, C., Lee, J., Shackelford, C., Edil, T., 2005. Long-term hydraulic conductivity of a non-prehydrated geosynthetic clay liner permeated with inorganic salt solutions. J. Geotech. Geoenviron. 131 (4), 405–417.

Koerner, R., 1998. Designing with Geosynthetics, fourth ed. Prentice Hall, Englewood Cliffs, New Jersey.

Meer, S., Benson, C., 2007. Hydraulic conductivity of geosynthetic clay liners exhumed from landfill final covers. J. Geotech. Geoenviron. 133 (5), 550–563.

Melchior, S., 1997. In-situ studies on the performance of landfill caps. In: Proc. International Containment Technology Conference. Florida State University, Tallahassee, FL, pp. 365–373.

Melchior, S., 2002. Field studies and excavations of geosynthetic clay barriers in landfill covers. In: Zanzinger, H., Koerner, R., Gartung, E. (Eds.), Clay Geosynthetic Barriers. Swets and Zeitlinger, Lesse, pp. 321–330.

Reitz, L., Holtz, R., 1997. Performance of Geotextiles in Landfill Covers, Proc. Geosynthetics '97. Industrial Fabrics Association International, St. Paul, MN, pp. 413–424.

Rowe, R., Sangam, H., Lake, C., 2003. Evaluation of an HDPE geomembrane after 14 years as a leachate lagoon liner. Can. Geotech. J. 40, 536–550.

Scalia, J., Benson, C. Preferential flow in geosynthetic clay liners exhumed from final covers with composite barriers. Can. Geotech. J., in press.

Shackelford, C., Benson, C., Katsumi, T., Edil, T., 2000. Evaluating the hydraulic conductivity of GCLs permeated with non-standard liquids. Geotext. Geomembranes. 18 (2–3), 133–161.

Stark, T., Williamson, T., Eid, H., 1996. HDPE geomembrane/geotextile interface shear strength. J. Geotech. Geoenviron. 122 (3), 550–563.